Articles

(Tetrakis(2-pyridylmethyl)ethylenediamine)iron(II) Perchlorate. Study of Density Functional Methods

Guangju Chen,[†] G. Espinosa-Perez,[‡] A. Zentella-Dehesa,[‡] I. Silaghi-Dumitrescu,[‡] and F. Lara-Ochoa*,[‡]

Chemistry Department, Beijing Normal University, Beijing 100875, China, and Instituto de Quimica, Universidad Nacional Autonoma de Mexico, Ciudad Universitaria, Coyoacan, 04510 Mexico D.F., Mexico

Received June 11, 1999

On the basis of the data obtained by X-ray diffraction, the properties of two independent crystallographic subsystems in the $[Fe(tpen)](ClO_4)_2 \cdot {}^2/_3H_2O$ complex are studied in detail with the density functional method B3LYP. The energies of singlet, triplet, and quintet states at different temperatures are obtained, the influences of geometry on energy changes are analyzed, the regularity of the spin-state interconversions is investigated, and the effect of the triplet and action of the anion on spin crossover are discussed. This investigation demonstrates that (1) the energy difference between the high-spin state and singlet state decreases as the Fe−N distance and geometric distortion increase, (2) the spin-equilibrium system is predominantly in low-spin form below room temperature and the proportion of high-spin state rapidly increases above room temperature, (3) one of the two cation sites has a greater presence of the high-spin content, (4) the triplet state may be responsible for the fast rate of spin-state interconversions, and (5) the B3LYP method proves to be very adequate to study the spin-state transition of this complex.

Introduction

The temperature-dependent spin-state interconversions in transition-metal complexes have been the subject of rather extensive studies for many years.[1−4] In these investigations various physical techniques have been employed such as crystal structure determinations, light-induced excited-spin-state trapping (LIESST),[5] the laser flash-photolysis technique (LFPT),[6] Fourier transform infrared spectroscopy (FTIP),[7] electronic spectra,[8] and Mössbauer spectroscopy and magnetic susceptibility measurements.[9] Insightful knowledge on spin-state interconversion can be obtained by using these experimental techniques. For instance, the temperature variation of magnetic susceptibility is the classical and the most direct macroscopic criterion, while Mössbauer spectroscopy has been the preferred technique to provide a microscopic criterion for spin equilibrium,[2] the geometric change accompanying the spin-state transition can be observed with X-ray crystallography, and the relaxation kinetics of the spin-crossover complex can be studied by LFPT. As a powerful complementary investigation method to experimental techniques, ab initio and DFT methods have also been used to study these systems.[10,11] The advantages of the computational methods are that they provide detailed information on the influence of molecular geometry on energy changes as well as the electronic distribution and other properties. This will allow us to better understand the spin-state transitions from a microscopic point of view.

In this paper, we report in detail the investigation results of the $[Fe(tpen)](ClO_4)_2$ complex (tpen = (tetrakis(2-pyridylmethyl)ethylenediamine) using the density functional method DFT/B3LYP[12] and also briefly describe the X-ray structural characterization of this complex. Experimental studies of this complex in some temperatures have been carried out previously.[9,13−16] However, the crystal structural data in low temperature have not been reported; especially many questions with regard

[†] Beijing Normal University.
[‡] Universidad Nacional Autonoma de Mexico.

(1) Beattie, J. K. *Advances in Inorganic Chemistry*; Academic Press Inc.: San Diego, CA, 1988; pp 32, 1−53.
(2) Toftlund, H. *Coordination Chemistry Reviews*; Elsevier Science Publishers B.V.: Amsterdam, 1989; Vol. 94, p 67.
(3) Konig, E. *Struct. Bonding* **1991**, *76*, 51−152.
(4) Gutlich, P.; Hauser, H.; Spiering, H. *Angew. Chem., Int. Ed. Engl.* **1994**, *33*, 2024.
(5) Hinek, R.; Spiering, H.; Schollmeyer, D.; Gutlich, P.; Hauser, A. *Chem. Eur. J.* **1996**, *2*, 1435.
(6) Conti, A. J.; Xie, C.-L.; Hendrickson, D. N. *J. Am. Chem. Soc.* **1989**, *111*, 1171.
(7) Herber, R. H. *Inorg. Chem.* **1987**, *26*, 173.
(8) Christiansen, L.; Hendrickson, D. N.; Toftlund, H.; Wilson, S. R.; Xie, C.-L. *Inorg. Chem.* **1986**, *25*, 2813.
(9) Chang, H. R.; McCusker, J. K.; Toftlund, H.; Wilson, S. R.; Trautwein, A. X.; Winkler, H.; Hendrickson, D. N. *J. Am. Chem. Soc.* **1990**, *112*, 6814.
(10) Xu, Zh.; Lin, Zh. *Chem. Eur. J.* **1998**, *4*, 28.
(11) Havlin, R. H.; Godbout, N.; Salzmann, R.; Wojdelski, M.; Arnold, W.; Schulz, C. E.; Oldfield, E. *J. Am. Chem. Soc.* **1998**, *120*, 3144.
(12) Becke, A. D. *J. Chem. Phys.* **1993**, *98*, 5648.
(13) Anderegg, G.; Wenk, F. *Helv. Chim. Acta* **1967**, *50*, 2330; *Chimia* **1970**, *24*, 427.
(14) Boggess, R. K.; Hughes, J. W.; Chew, C. W. *J. Inorg. Nucl. Chem.* **1981**, *43*, 939.
(15) Toftlund, H.; Yde-Andersen, S. *Acta Chem. Scand., Ser. A* **1981**, *35*, 575.
(16) Solans, X.; Ruiz-Ramirez, L.; Moreno-Esparza, R.; Labrador, M.; Escuer, A. *J. Solid State Chem.* **1994**, *109*, 315.

10.1021/ic990676z CCC: $19.00
Published on Web 07/12/2000

to the spin-state interconversion of this complex remain to be answered theoretically. Because this is the very significant spin-state interconversion example of an iron(II) complex system directly studied by the computational method on the basis of experimental data at different temperatures, we attempt to address the following aspects in this study: (1) the energy changes of the complex versus temperature; (2) the influences of geometric structure on the energy difference between the different spin states; (3) the peculiarity of the spin-state interconversions; (4) the influence of the anion and the important effect of the triplet on the spin-state interconversion; (5) the reason for the spin-state transition.

Computational Method

The geometric data of the $[Fe(tpen)](ClO_4)_2$ complex, consisting of two independent crystallographic molecules at different temperatures (120, 150, 223, 293, and 358 K), are obtained by X-ray crystallography. Because the complete system contains too many atoms for our calculations, especially heavy atoms, only two subsystems are investigated, which are here referred to as sites A and B. One of the best methods to study the spin-crossover system of the transition-metal complex is the multiconfigurational self-consistent field (MCSCF), including complete active space SCF(CASSCF)[17] or multireference configuration interaction (MR-CI);[18] unfortunately sites A and B are still too large for this type of calculation. From a practical and economical point of view, therefore, we resorted to a density functional method (B3LYP), which has been shown to yield quite accurate results for the energy and geometry of transition-metal compounds.[19] The B3LYP[12] is a Beck three-parameter hybrid method using the Lee−Yang−Parr correlation function[20] which includes both local and nonlocal terms, and a Vosko−Wilk−Nusair correlation function[21] referred to as a local spin density correlation. We used a split valence basis set 3-21G[22] with six Cartesian d orbitals for all electrons of the Fe atom. To discuss the effect of basis set, the following basis set was used to study the spin-state transitions of some temperatures: a 6-311g-(d) basis for all electrons of iron[23] and for all atoms directly bonded to iron, and a 6-31g basis for all other atoms. The following several sets of calculations have been carried out using UB3LYP/3-21G. Two crystallographically different $[Fe(tpen)]^{2+}$ cations as well as the corresponding neutral $[Fe(tpen)](ClO_4)_2$ molecules are studied. In each case, singlet (S), triplet (T), and quintet (Q) states are considered separately. All calculations were performed using the Gaussian 94 program[24] on the supercomputer of UNAM.

Results and Discussion

1. Geometric Characteristics of the Complex. The X-ray crystal diffraction experiment shows that the $[Fe(tpen)](ClO_4)_2 \cdot {}^2/_3H_2O$ complex crystallizes in the monoclinic space group $C2/c$ and there are two independent crystallographic molecules in the temperature region studied. Estimated standard deviations of X-ray structure determination for the last significant figure are about 0.00002−0.00008 for the positional parameters. The view of the complex molecule in Figure 1 shows that the two $[Fe(tpen)]^{2+}$ cations have a distorted octahedral coordination geometry, with two aliphatic (N3 and N6 for site A or N10 and N11 for site B) and four aromatic nitrogen atoms comprising the 6N coordination sphere.

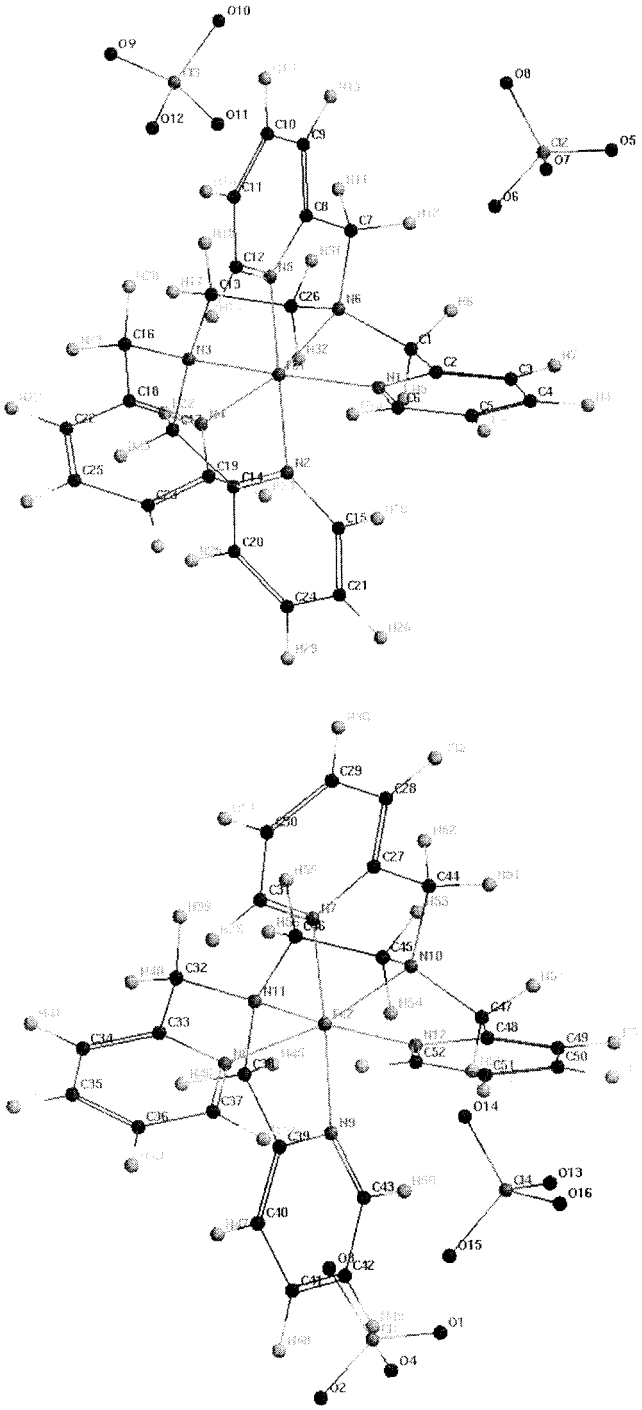

Figure 1. Molecular structure and labeling of $[Fe(tpen)](ClO_4)_2$ molecules: (a, top) site A, (b, bottom) site B.

The two important structural features, which determine the properties of the iron(II) complex, are the metal−ligand distance and the distortion of the coordination polyhedron. The distortion is usually described by the twist angle (ϕ) between the two opposite trigonal faces.[2,9] For a strict octahedron, the twist angle ϕ is 60°. If the two trigonal planes, which are N2−N3−N4 and

(17) Shepard, R. In *Advances in Chemical Physics ab initio method in Quantum Chemistry II*; Lawleg, K. P., Ed.; John Wiley & Sons. Inc.: New York, 1987; p 63.
(18) Shavitt, I. In *Modern Theoretical Chemistry, 3: Method of Electronic Structure Theory*; Schaefer, H. F., III, Ed.; Plenum: New York, 1977; p 189.
(19) Siegbahn, P. E. M. In *Advances in Chemical Physics XCIII: New methods in Computational Quantum Mechanics*; Prigogine, I., Rice, S. A., Eds.; John Wiley & Sons Inc.: New York, 1996; p 333.
(20) Lee, C.; Yang, W.; Parr, R. G. *Phys. Rev. B* **1988**, *37*, 785.
(21) Vosko, S. H.; Wilk, L.; Nusair, M. *Can. J. Phys.* **1980**, *58*, 1200.
(22) Pietro, W. J.; Francl, M. M.; Hehre, W. J.; Defrees, D. J.; Pople, J. A.; Binkley, J. S. *J. Am. Chem. Soc.* **1982**, *104*, 5039.
(23) Wachters, A. J. H. *J. Chem. Phys.* **1970**, *52*, 1033.
(24) Gaussian 94: Frisch, M. J.; Trucks, G. W.; Schlegal, H. B.; Gill, P. M. W.; Johnson, B. G.; Robb, M. A.; Cheeseman, J. R.; Keith, T. A.; Petersson, G. A.; Montgomery, J. A.; Raghavachari, K.; Al-Laham, M. A.; Zakrzewski, V. G.; Ortiz, J. V.; Foresman, J. B.; Cioslowski, J.; Stefanov, B. B.; Nanayakkara, A.; Challacombe, M.; Peng, C. Y.; Ayala, P. Y.; Chen, W.; Wong, M. W.; Andres, J. L.; Replogel, E. S.; Gomperts, R.; Martin, R. L.; Fox, D. J.; Binkley, J. S.; Defrees, D. J.; Baker, J.; Stewart, J. P.; Head-Gordon, M.; Gonzalez, C.; Pople, J. A., Gaussian, Inc., Pittsburgh, PA, 1995.

Table 1. Average Trigonal Twist Angles (deg) at Different Temperatures

	site A		site B	
T (K)	type I	type II	type I	Type II
120	49.62	70.38	47.36	72.64
150	49.48	70.52	47.35	72.65
223	49.13	70.87	47.37	72.63
293	49.07	70.93	46.02	73.98
358	46.65	73.35	42.49	77.51

Table 2. Average $Fe-N_{aliph}$ and $Fe-N_{py}$ Distances (Å) at Different Temperatures

	site A		site B	
T (K)	$Fe-N_{aliph}$	$Fe-N_{py}$	$Fe-N_{aliph}$	$Fe-N_{py}$
120	2.051	2.000	2.021	2.014
150	2.044	1.994	2.019	2.011
223	2.033	1.986	2.016	2.006
293	2.020	1.975	2.020	2.037
358	2.092	2.033	2.088	2.055

N1−N5−N6 for site A, and N7−N10−N12 and N8−N9−N11 for site B, are defined, two different types of twist angles (types I and II) are identified. In Table 1, the two different types of average trigonal twist angles at 120, 150, 223, 293, and 358 K are listed.

Therefore, there are different degrees of trigonal distortion in sites A and B. The absolute differences ($\Delta\phi$) between the twist angle of the complex and the ideal octahedron proportionally correspond to a distortion of the complex. $\Delta\phi$ is thought to be substantial trigonal distortion. The data in Table 1 show that the degree of distortion is larger for site B than for site A, at different temperatures. For example, $\Delta\phi$ is about 13.35° for site A and 17.51° for site B at 358 K. The trigonal distortion increases as the temperature rises, and the changing degree of distortion is very small below 293 K ($\phi < 1°$) but becomes larger above room temperature.

For Fe−N bond distances, $Fe-N_{aliph}$ and $Fe-N_{py}$ distances are different at all temperatures, even for cis and trans $Fe-N_{py}$ bond distances. But only the average $Fe-N_{aliph}$ and $Fe-N_{py}$ distances are given in Table 2 at five different temperatures. The average $Fe-N_{aliph}$ distance is larger than the average $Fe-N_{py}$ distance at all temperatures. Qualitatively, the variation in the Fe−N bond length is somewhat similar for both sites, showing a minimum at about room temperature for site A, and at lower temperature (223 K) for site B. A relatively large elongation for both cases is also noted at 358 K.

For the sake of clarity and simplicity, we only listed the average $Fe-N_{aliph}$ and $Fe-N_{py}$ distances and the average trigonal twist angles. But we stress here that there are indeed certain differences of geometric structure at different temperatures. Both radial and angular deformations are reflected in the energy change discussed in the following sections.

2. Energy Analysis. The energies of two crystallographically different $[Fe(tpen)](ClO_4)_2$ molecules and $[Fe(tpen)]^{2+}$ cations at 120, 150, 223, 293, and 358 K are summarized in Table 3. The plots of the relative energy (RE) for the two sites versus temperature are given in Figures 2 and 3. The RE is defined as the energy difference between the singlet state at 120 K and other spin states at the same or different temperatures ($RE = E_{other} - E_{singlet,120K}$).

The change of energy versus temperature for both sites obtained by UB3LYP/3-21G calculations shows the following trends: (1) The energy of the complex molecule or cation rises as temperature increases, and the increase of energy is greater for site A than for site B. (2) The singlet state has the lowest energy, followed by the quintet state, for the two different sites at the same temperature. Therefore, the spin-state transformations of this complex should be between singlet and quintet. (3) The changing trend of energy versus temperature is different for two sites, and the energy of high-spin states is closer to that of the singlet states for site B than for site A. (4) With rising temperature, the energy of the singlet state increases rapidly, and that of the quintet state tends to be smooth and steady in ionic states, especially at higher temperature.

The energy differences between molecules are greater than the energy difference in the ionic states at different temperatures. For example, the difference between singlet states for site B at 120 and 293 K is 1588.1 kJ/mol in the molecular case and 66.1 kJ/mol in the ionic case. Furthermore, in the molecular states the energy is much lower for site B than for site A in equal spin states and at the same temperature. However, the contrary is observed in the ionic states. The phenomena are actually caused by the anion of the system. In Table 4, the energies (E_{anion}) and relative energies (ΔE_{anion}) of anions for the two sites at 120, 150, 223, and 293 K are given.

These results show that when temperature is increased, E_{anion} for sites A and B also increases. However, the energy of the anion at 120, 150, 223, and 293 K for site B is always much lower than for site A at the same temperatures. The reason for this difference is probably that the Cl−O bond lengths and Cl−Cl distances are longer at low temperature than at high

Table 3. Energies (hartrees) of Molecules and Cations for the Two Sites

		molecular state		ionic state	
T (K)	multiplicity	site A	site B	site A	site B
	singlet	−4 099.573 38	−4 099.627 63	−2 586.183 12	−2 586.178 40
120	triplet	−4 099.535 39	−4 099.602 92	−2 586.159 76	−2 586.153 59
	quintet	−4 099.550 02	−4 099.612 37	−2 586.164 71	−2 586.163 25
	singlet	−4 099.471 72	−4 099.552 63	−2 586.182 59	−2 586.178 83
150	triplet	−4 099.438 61	−4 099.525 14	−2 586.156 96	−2 586.153 12
	quintet	−4 099.441 66	−4 099.536 02	−2 586.158 18	−2 586.161 97
	singlet	−4 099.227 28	−4 099.354 96	−2 586.183 25	−2 586.181 27
223	triplet	−4 099.191 67	−4 099.326 84	−2 586.155 59	−2 586.155 16
	quintet	−4 099.197 14	−4 099.335 77	−2 586.155 32	−2 586.161 22
	singlet	−4 098.862 03	−4 099.022 77	−2 586.164 41	−2 586.153 24
293	triplet	−4 098.809 85	−4 098.999 67	−2 586.118 38	−2 586.132 18
	quintet	−4 098.818 82	−4 099.012 81	−2 586.131 90	−2 586.142 82
	singlet			−2 586.125 45	−2 586.126 93
358[a]	triplet			−2 586.104 81	−2 586.111 69
	quintet			−2 586.126 46	−2 586.136 44

[a] No data available for the $(ClO_4)^-$ anion at 358 K.

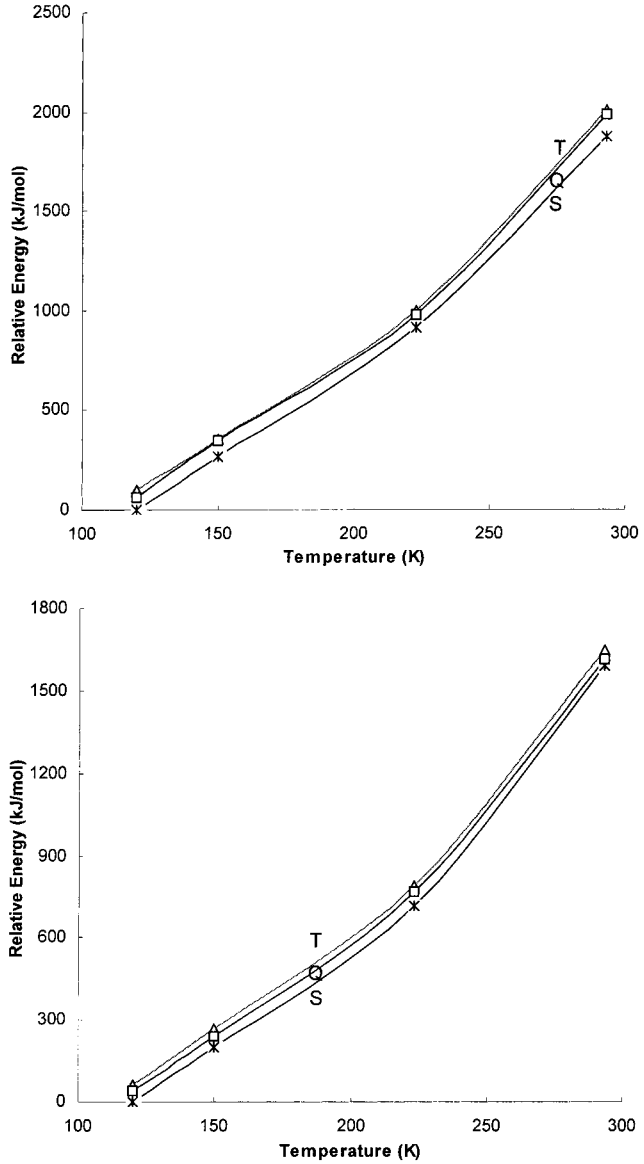

Figure 2. Energy versus temperature in molecular states: (a, top) site A, (b, bottom) site B.

temperature for the two sites; at the same temperature the Cl−O bond lengths and Cl−Cl distances are longer at site B than at site A. For example, the Cl−O average bond lengths are 1.457 Å (120 K) and 1.407 Å (293 K) for site B, but the values are 1.422 Å (120 K) and 1.357 Å (293 K) for site A. In addition,

Table 4. E_{anion} (hartrees) and ΔE_{anion} (kJ/mol) of Anions at 120, 150, 223, and 293 K

	site A		site B	
T (K)	E_{anion}	ΔE_{anion}	E_{anion}	ΔE_{anion}
120	−1 513.003 20	0.0	−1 513.082 75	0.0
150	−1 512.903 32	260.292	−1 513.006 47	200.273
223	−1 512.664 06	890.413	−1 512.807 31	723.168
293	−1 512.326 90	1775.627	−1 512.504 89	1517.173

the angle ∠Cl−O−Cl also affects the energy, and the larger the absolute difference between the angle and 109°28′, the higher the total energy. Thus, the molecular system has a much higher energy at high temperature than at low temperature because of the influence of the anion energy. The total energy is lower for site B than for site A in the molecular state for the same reason. However, a common characteristic in the molecular and ionic cases is that the energy difference between the high-spin state and singlet state is smaller for site B than for site A at the same temperature. Therefore, the energy difference among different spin states at the same temperature is naturally consistent.

Usually, the unrestricted Hartree−Fock wave function is no longer a true eigenfunction of the total spin operator because the state of high spin multiplicity will be mixed into the low-spin state. Therefore, we must inspect the extent of such a spin "contaminant" so as to determine whether these energies obtained by a single determinant wave function are reasonable by examining the expectation value of the operator $\langle S^2 \rangle$. For singlet states, the expectation values of $\langle S^2 \rangle$ at different temperatures are approximately zero. The calculated expectation values of $\langle S^2 \rangle$ of triplet and quintet states are about 2.06 and 6.12 at different temperatures. These values decrease as the temperature rises. Further, the expectation values of $\langle S^2 \rangle$, after annihilation of the first spin contaminant estimated by calculations, are about 2.0010 for the triplet states and 6.0005 or so for the quintet states. Although the spin contaminant of quintet states seems to be slightly large from the value, we think that the extent of the spin contaminant does not exert any influence on our conclusion because the change of E, resulting in the decrease of expectation values of $\langle S^2 \rangle$, is small. For example, when the expectation values of $\langle S^2 \rangle$ of site A at 358 K are 6.0969 and 6.0206, respectively, their energy difference is less than 2 kcal/mol. The energy of the quintet state is always lower than that of the triplet state in both cases. Another important fact is that the spin density is mainly distributed on the Fe atom of this complex and the spin density values of other atoms are smaller than 0.05. For example, the spin density of the Fe atom is 1.90−2.10 for the triplet state and 3.80−3.95 for the quintet

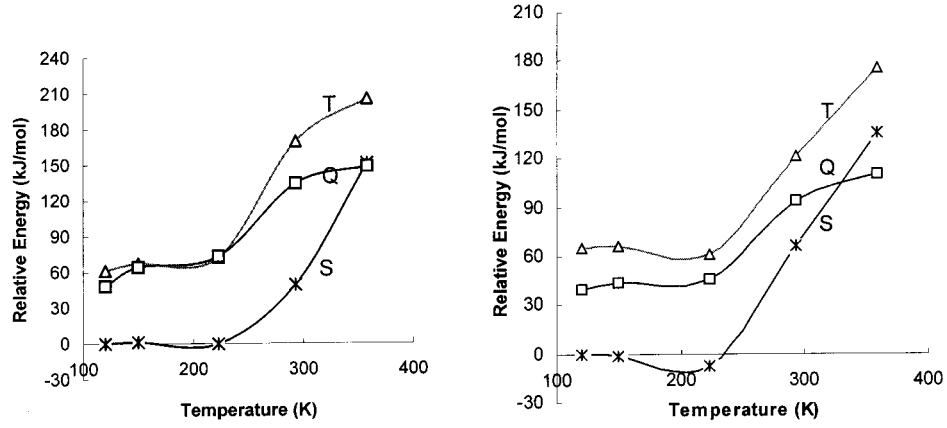

Figure 3. Relative energy versus temperature in ionic states: (a, left) site A, (b, right) site B.

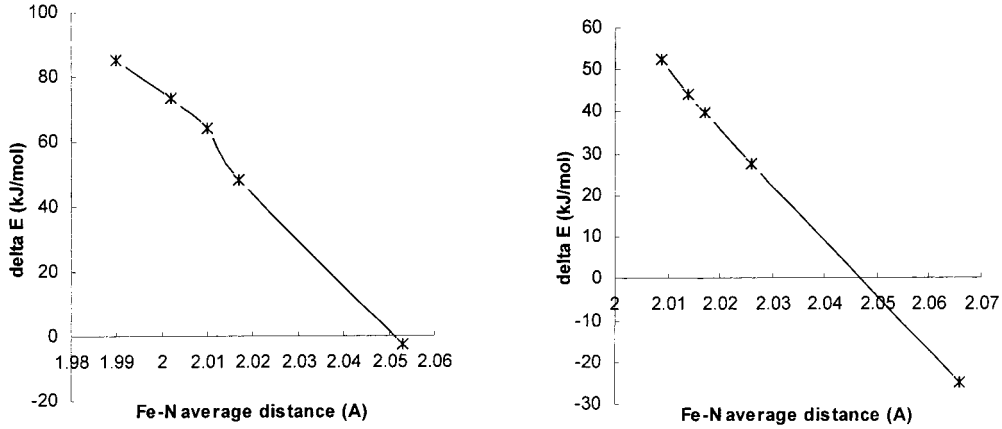

Figure 4. ΔE in ionic states versus the Fe−N average distance: (a, left) site A, (b, right) site B.

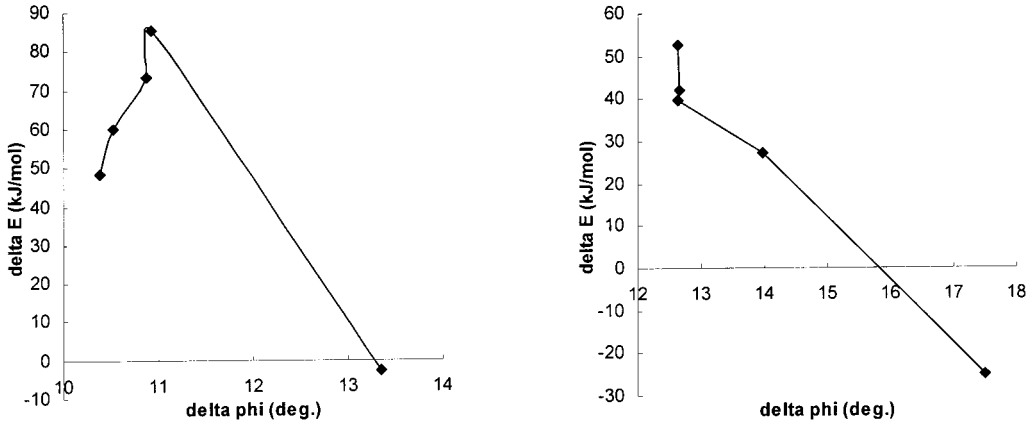

Figure 5. ΔE in ionic states versus $\Delta\phi$: (a, left) site A, (b, right) site B.

Table 5. ΔE (kJ/mol) between the Quintet and Singlet States

	molecular state		ionic state	
T (K)	site A	site B	site A	site B
120	61.086	40.166	48.335	39.772
150	78.923	43.609	64.089	44.266
223	79.133	50.383	73.357	52.484
293	113.448	26.150	85.355	27.358
358			−2.651	−24.968

state, and is basically concentrated on the d orbitals of the Fe atom. Therefore, we believe that the energies obtained by UB3LPY/3-21G are reliable, most likely due to the fact that the method takes local and nonlocal electron correlation into account in an explicit manner.

3. Energy Change and Spin-State Transitions. Typically, there are two different types of spin-state transitions: (1) an abrupt transition, which occurs at a well-defined transition temperature (T_c); (2) a gradual transition, which occurs over a broad temperature range, and whose critical temperature T_c is defined by the temperature where the high-spin fraction n_{HS} is equal to 0.5. According to the μ_{eff} versus temperature curve, one may describe the spin-state transition in the [Fe(tpen)]-$(ClO_4)_2$ complex as a gradual transition.[9] Because the spin-state transition is actually related to the energy difference between the high-spin state and singlet state, the energy difference (ΔE) between the quintet and singlet at the same temperature is shown in Table 5.

ΔE between the quintet and singlet is strongly temperature-dependent and thus geometry-dependent. Actually, the spin change is always accompanied by geometrical changes in the ligand sphere around the iron ion. These changes are observed both in the Fe−N bond distance and in the trigonal distortion movement of the coordination polyhedron.

First, the longer the Fe−N bond distance, the smaller the absolute ΔE between the quintet state and singlet state. For example, ΔE for site A increases as the Fe−N distances are shortened within the temperature range of 120−293 K; then ΔE rapidly decreases at 358 K due to the elongation of the Fe−N distances. Similarly, ΔE for site B at 223 K is larger because the Fe−N distance is shorter at this temperature (cf. Table 2). Plots of ΔE of the quintet state and singlet state versus the Fe−N average distance for the two forms of cations are given in Figure 4. The plots for the two sites show that the Fe−N average distance dependence of ΔE is almost linear; i.e., the increasing distance leads rapidly to a decrease in ΔE. Therefore, it may be concluded that a change in the metal−ligand distance is a crucial parameter in predicting spin-state change.

Second, the larger trigonal distortion $\Delta\phi$ corresponds to a smaller ΔE between the quintet and singlet states. Figure 5 illustrates the relationship between ΔE and $\Delta\phi$. In contrast with Figure 4, the $\Delta\phi$ variation does not have a linear relationship with ΔE, and it shows an abnormal behavior in the region of $\Delta\phi = 10-11°$ for site A and about 12.64° for site B. Actually, these plots reflect a compromise between Fe−N distance changes and the trigonal distortion effects (cf. Tables 1 and 2). For site A, the trigonal distortion $\Delta\phi$ increases 0.55°, but Fe−N_{aliph} and Fe−N_{py} average lengths decrease to 0.031 and 0.025 Å, respectively, in the temperature ranges from 120 to 293 K. For site B, there is a very small change (0.01°) of the trigonal distortion $\Delta\phi$, but the Fe−N distances are shortened from 120 to 223 K. The decreases of the Fe−N distance and increases of

Table 6. Interaction Energies (kJ/mol) between the Anion and Cation

	site A		site B	
T (K)	singlet	quintet	singlet	quintet
120	−1016.227	−1003.231	−962.194	−961.905
150	−1012.945	−998.111	−964.425	−965.082
223	−997.612	−991.820	−961.931	−964.189
293	−973.326	−945.233	−957.363	−958.571

the trigonal distortion will exert an opposing effect on the change of ΔE, and the result is that the former has more impact than the latter. When the temperature is higher than room temperature, there is an approximately linear relationship between the trigonal distortion and ΔE, too.

Third, at the same temperature, ΔE is smaller for site B than for site A in the molecular and/or ionic states due to the fact that the Fe−N average bond distance and trigonal distortion of site B are greater than those of site A.

Fourth, the energy of the quintet state is lower than that of the singlet state for the two sites at temperatures of about 358 K from Table 5. The rapid decrease of ΔE above room temperature is consistent with the increase of the Fe−N average bond distance and trigonal distortion.

Fifth, a measure of the influence of the anion on the energy, in different spin states, might be the interaction energy (IE) defined as the energy of the molecule minus the energy sum of the cation and anion [$IE = E_{molecule} - (E_{anion} + E_{cation})$]. In Table 6, the interaction energies between the anion and cation at 120, 150, 223, and 293 K are listed. Since the interaction energies between the cation and anion for the singlet and quintet states are different, they will play a specific role in changing the singlet−quintet ΔE. As shown in Table 6, the interaction will generally favor the spin-state transition for site B due to the decrease in ΔE, but this is disadvantageous for site A. It should also be indicated that the local environment around the cation is not fully considered in our calculations because of the large system. Nonetheless, it is clear that ΔE will change due to the presence of the anion. Furthermore, anions will also exert influence on the geometric structure of the cations. Thus, the spin-state transition is partially influenced by the anion. In fact, salts of the cation $[Fe(tpen)]^{2+}$ with PF_6^-, BPh_4^-, and Br^- exhibit magnetic characteristics of low spin up to 350 K.[2]

Since the spin-state transition is closely related to the energy change in different spin states, from the above discussion we may further deduce certain peculiarities of the spin-state interconversion for this complex according to the relationship of particle number distributions and energy. (1) As shown in Figure 3, two crystallographically different sites do not act simultaneously in high/low-spin-state interconversion due to the different changing trend of energy versus temperature. But the two subsystems undergo a gradual spin-state transition, because the change of energy difference between the high-spin state and the singlet state versus temperature is gradual; i.e., it is a spin equilibrium system thermally. (2) The complex system is predominantly in the low-spin form below room temperature, due to larger energy differences between the singlet state and the quintet state (27.4 kJ/mol at least). (3) The fraction of high-spin state rapidly increases as the Fe−N bond distance and the trigonal distortion increase because the energy difference between the singlet state and the quintet state decreases rapidly in this case. (4) The high-temperature structure represents the increase of the contribution from the high-spin form. For example, the high-spin form has been predominant for site B at 358 K. (5) The system reflects more high-spin fraction at different temperatures for site B than for site A, and only site B may reflect a high-spin component at about 300 K, because of the decreasing energy difference between the quintet and singlet (ΔE = 27.4 kJ/mol at 293 K). These conclusions are very consistent with the experimental facts.[9,16]

As the high-spin geometry is not experimentally available, a calculation of two geometries in the ionic state of sites A and B was made. The ZINDO/1 method was used to explore the structure of the high-spin state because the system is large. When the starting temperature was 358 K and the simulation temperature 420 K, the Monte Carlo method was first used to search for the conformation on the basis of the structure at 358 K. Then the conformations corresponding to two different minima were further obtained in a full geometry optimization by the ZINDO/1 method. In these geometries, the average trigonal twist angles and the average Fe−N distances are 46.37° and 2.143 Å (site A) and 39.77° and 2.141 Å (site B), respectively. For site A, the energies of the singlet and quintet states are −2 586.136 10 and −2 586.169 28 hartrees, and the energies for site B are −2 586.124 06 and −2 586.162 07 hartrees, respectively. In two cases, the energies of the quintet state are much lower (at least 87 kJ/mol) than those of the singlet state. Obviously, the high-spin form is absolutely predominant in the two geometry structures. Hence, we may take these geometries as those of the quintet states. This fact further shows that the high-spin fraction increases as the Fe−N distance and geometric distortion increase.

It should be pointed out that there was a quantitative discrepancy between computation and experiment. The results obtained by UB3LYP/3-21g* showed that the intersection of the energy curve of the singlet and quintet states is about 350 K (site A) or 330 K (site B). However, the critical temperature T_c, where there are equal amounts of high- and low-spin complexes, is 365 K experimentally. To inspect the effect of basis set, two molecular cation subsystems of 223 and 358 K were calculated by using a 6-311g(d) basis for all electrons of iron and for all atoms directly bonded to iron, and a 6-31g basis for all other atoms. The results are given in Table 7. Some results obtained by the basis sets are similar to results by 3-21g*. For example, the energy is lower for site B than for site A, and the energy difference between the singlet state and the quintet state is larger at 233 K than at 358 K, and so on. But the energy of the quintet state is still higher, at least 52 kJ/mol, than that of the singlet state at 358 K. The result shows that the complex system is predominantly in the low-spin form even at this temperature. Obviously, this fact is also not in agreement with the experimental results that μ_{eff} (μ_B) is larger than 3.2 at 358 K. As regards the geometries obtained by calculations, the energy differences between the quintet and singlet states are −11.79 (site A) and −41.04 (site B) kJ/mol, respectively; i.e., the energy of the quintet state is lower than that of the singlet state. However, the larger basis set we used, as a whole, seems not to be suitable for the discussions on the spin-state transition of the system. The computational method is perhaps more important than the effect of basis set, and either a complete system should be calculated or a better basis set should be used. It is very difficult from the present computational condition.

The experimental results show that the $[Fe(tpen)](ClO_4)_2$ complex is a ferrous system with a faster rate of interconversions between high- and low-spin states than can be detected by the Mössbauer technique.[9] The fast spin-state interconversion may be related to an increased spin−orbit coupling. In the case of the octahedral iron(II) spin-crossover complex, the $^1A_1$ ground state and $^5T_2$ high-spin state are not mixed directly by the spin−

Table 7. Energy (hartrees) and ΔE (kJ/mol) Obtained Using a Large Basis Set[a]

	site A			site B		
T (K)	S	Q	ΔE_{Q-S}	S	Q	ΔE_{Q-S}
223	−2 599.297 19	−2 599.240 66	148.4	−2 599.295 86	−2 599.245 57	132.0
358	−2 599.247 48	−2 599.218 22	76.8	−2 599.251 45	−2 599.231 71	51.8

[a] S = singlet; Q = quintet.

Table 8. Energy Difference (kJ/mol) between the Triplet State and Singlet State

	molecular state		ionic state	
T (K)	site A	site B	site A	site B
120	99.743	64.852	61.332	65.139
150	86.930	72.175	67.292	67.502
223	93.494	73.829	72.621	68.552
293	136.999	60.649	120.852	55.739
358			54.190	40.013

orbit coupling, and they are involved in a spin−orbit interaction via the $^3T_1$ and/or $^3T_2$ state. Thus, the energy of the triplet is important to evaluate the extent of mixing of the singlet and quintet states. Although the spin−orbit interactions cannot directly be discussed from our calculations, some information can be obtained from the change of the triplet energy at different temperatures. Table 8 lists the absolute values of the energy difference between the triplet state and the singlet state.

From our results it is clear that the triplet energy is close to the singlet energy when the trigonal distortion is great and the Fe−N bond distance is long. Conversely, the difference between the triplet and singlet energies is great when trigonal distortion is small and the Fe−N bond distance is short. This is probably because a trigonal distortion is induced by the tpen ligand, and the long Fe−N distance contributes to a significant stabilization of the intermediate triplet state. Lowering the energy of the triplet state should have the same net effect as the increase in spin−orbit coupling because, according to the perturbation theory, the mixing between the quintet and singlet states depends on the square of the energy difference between the singlet and triplet states.[1] Thus, an increased spin admixture of the singlet/quintet with the intermediate excited triplet state will result in an increased rate of spin-state interconversion. Again, the smallest difference between the singlet and triplet states appears at high temperature, especially for site B, which suggests that it is more active for the quintet−singlet interconversions at this temperature. Therefore, we think that the triplet state plays an important role in spin-state interconversion of the [Fe(tpen)]-$(ClO_4)_2$ complex.

4. Further Discussion. For a spin-equilibrium system, our main result for a spin-state transition from computational data is that the energy of the high-spin state gradually approximates that of the low-spin state, when the temperature is changed. The tendency of energy change should be closely related to the electronic distributions and molecular orbital interactions in different spin states. Therefore, it is necessary to discuss and compare the orbital interaction and electronic densities of different spin states to reveal a spin-change process with more detail. For this reason, molecular orbitals (MOs) and Mülliken populations are calculated, and some higher occupied MOs and lower unoccupied MOs are analyzed in detail.

For singlet states, the higher occupied MOs include mostly the d_{xy}, d_{xz}, and d_{yz} atomic orbitals (AOs) of the Fe atom, and the overlaps between the Fe and ligand orbitals in these MOs are not great. The orbital energies (ϵ) of the highest three α and three β occupied MOs rise gradually as the geometric distortion and Fe−N average distance increase. Similarly, the orbital energies of the lower unoccupied MOs, including the $d_{x^2-y^2}$ and d_{z^2} orbitals of the Fe atom, drop as the geometric distortion and Fe−N average distance increase. This is because the orbital overlap between Fe and the ligand is diminished as the large distortion and Fe−N distance increase. Therefore, the orbital energy differences ($\Delta\epsilon$) between the occupied and unoccupied MOs will decrease. For site A, we have the sequence $\Delta\epsilon_{358K} < \Delta\epsilon_{120K} < \Delta\epsilon_{150K} < \Delta\epsilon_{223K} < \Delta\epsilon_{293K}$, and $\Delta\epsilon_{358K} < \Delta\epsilon_{293K} < \Delta\epsilon_{120K} < \Delta\epsilon_{150K} < \Delta\epsilon_{223K}$ for site B in turn. These orders are completely consistent with the changing trend of ΔE (cf. Table 5). For example, $\Delta\epsilon$ is 5.313 eV at 358 K and 5.571 eV at 120 K for site B and 5.537 eV at 120 K and 5.687 eV at 293 K for site A in similar MOs. Thus, the decrease of $\Delta\epsilon$ will induce an electron transfer between different MOs easily. This may be one of the intrinsic reasons for the large trigonal distortion, and the Fe−N distance reflects more prominently the presence of the high-spin fraction.

The higher occupied MOs for the quintet state are different from those of the singlet state. These differences reside mainly in the contributions from all five independent d orbitals of the Fe atom, and the orbital overlaps between Fe and the ligands are greater for the quintet state than for the singlet state. It should be especially mentioned that MOs with $d_{x^2-y^2}$ and d_{z^2} have obvious properties of a σ-type MO, but MOs with d_{xy}, d_{xz}, and d_{yz} do not completely possess characteristics of a π MO due to geometric distortion. The orbital energies of these molecular orbitals decrease as the Fe−N distances increase, and this may be related to the delocalization of the electrons in the quintet state, because the proportion of higher energy AOs (*n*s, *n*p, and *n*d) in the MOs increases. This point is reflected by the fact that the electronic kinetic energy increases and the electron−electron repulsion energy decreases for the quintet state relative to the singlet state at the same temperature. A drop of five α and one β molecular orbital energies ϵ of the quintet state, especially ϵ relative to that of the singlet state, will result in a ΔE (the energy difference between the quintet and singlet states) decrease. For example, for site B, the sums of ϵ for the six higher occupied MOs with d AOs are −62.74 and −69.68 eV for the singlet state and quintet state at 120 K, with similar values of −62.59 and −70.59 eV at 358 K. Thus, their absolute differences are 6.94 eV at 120 K and 8.00 eV at 358 K, demonstrating that ΔE is smaller at 358 K than at 120 K. This might be another possible intrinsic reason to explain why the large Fe−N distances become more pronounced with a decrease in the energy difference between the quintet and singlet states.

From the electronic distributions point of view, the electronic population of 3d, 4s, and 4p AOs on the Fe atom is larger for long Fe−N distances than for short Fe−N distances. This result is in good agreement with the expected variation that a high-spin fraction should increase with an increases of the Fe−N distance. The electronic spin density of the high-spin state in the complex is almost distributed on the 3d atomic orbitals of the Fe atom and is close to zero on the other atoms. For the triplet state, the values of the electronic spin density are between 1.90 and 2.10, and these values are 3.80−3.95 for the quintet state.

Regardless of the singlet and quintet states, the charge on

Table 9. Final R (%) Values for $T = 120$, 150, 223, and 293 K

T (K)	R (%)	total no of reflns collected	no. of unique reflns (R_{int})	no. of obsd reflns ($F_o \geq 4\sigma F$)	range
120	5.51	17 522	17 522 (0.00)	11 919	$-27 \leq h \leq 46$, $-11 \leq k \leq 11$, $-30 \leq l \leq 24$
150	5.87	17 579	17 579 (0.00)	10 882	$-27 \leq h \leq 46$, $-11 \leq k \leq 11$, $-30 \leq l \leq 24$
223	6.09	17 753	17 753 (0.00)	9 651	$-27 \leq h \leq 47$, $-11 \leq k \leq 11$, $-30 \leq l \leq 24$
293	6.37	18 112	18 112 (0.00)	8 180	$-28 \leq h \leq 47$, $-10 \leq k \leq 11$, $-31 \leq l \leq 24$

Table 10. Crystal Parameters for the $[Fe(tpen)](ClO_4)_2 \cdot {}^2/_3H_2O$ Complex at Different Temperatures

T (K)	a (Å)	b (Å)	c (Å)	β (deg)	V (Å^3)	Z	μ(Mo Kα) (mm^{-1})
120	40.368(1)	9.422(0)	23.881(1)	108.841(0)	8596.11	12	0.78
150	40.391(2)	9.427(1)	23.850(1)	108.816(0)	8590.04	12	0.78
223	40.647 (3)	9.464 (1)	23.925 (1)	108.616(1)	8722.25	12	0.77
293	40.977(1)	9.450(1)	23.977(2)	108.329(1)	8860.12	12	0.75
358[a]	41.00(2)	9.517(5)	24.21(1)	109.46(4)	8905(15)	12	0.75

[a] Reference [9].

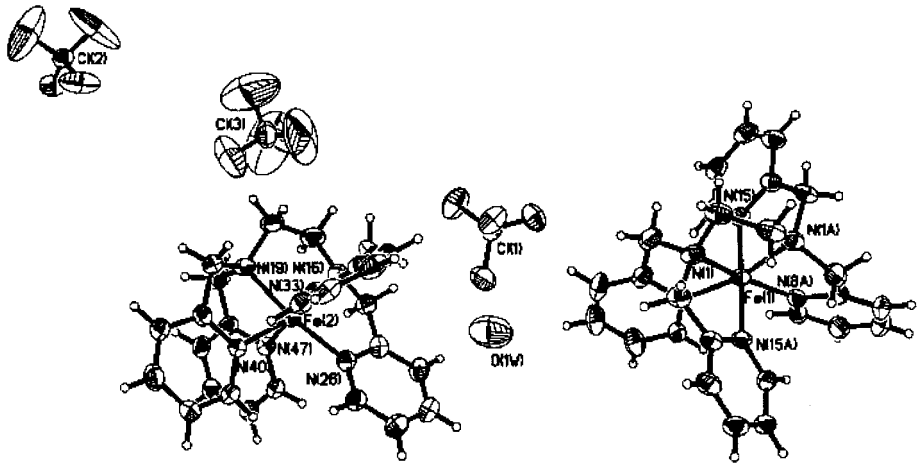

Figure 6. Molecular structure of $[Fe(tpen)](ClO_4)_2 \cdot {}^2/_3H_2O$ with ellipsoids drawn at the 50% probability level [symmetry code: (i) $-x, y, -z + 1/2$].

the Fe atom decreases as the trigonal distortion and Fe−N distances increase. For instance, the charges on Fe for the quintet state in site B are 1.526 at 223 K and 1.356 at 358 K. This shows that the larger the electronic population number on the Fe atom, the higher the high-spin fraction. The Fe−N bond electronic densities exhibit a similar regularity. Another interesting fact is that the positive charge of Fe is greater for the quintet state than for the singlet state at the same temperature. In fact, the overlaps between the d orbital of the Fe and the orbitals of the ligand are greater for the quintet state than for the singlet state, and these MOs are heavily weighted on the Fe atom. Thus, a small amount of electronic density for the quintet state is transferred from the Fe atom to the ligand. The increase of negative charges of the N atoms for the quintet state relative to the singlet state supports this viewpoint too.

4s and 4p AOs on the Fe atom also have an important effect on the spin-state transition from MO analysis and electronic distributions. For example, electronic populations on 4s and 4p AOs of the Fe atom are 0.759 77 and 0.815 64 for the singlet and quintet states of site B at 358 K.

The reason that the quintet state has lower energy than the triplet state at different temperatures may be related to the molecular orbital energy as well, because both the sum of the MO energies including the *d* orbitals of the Fe atom and the total orbital energy are lower for the quintet state than for the triplet state.

In summary, the energy-changing trend we have discussed here or spin-state interconversion is closely related to the orbital behavior and electronic distribution of different spin states. Because the results obtained with B3LYP/3-21g* give many changes in the regularity of the properties of the complex adapted to the geometric structure change, we consider the method very efficient and relatively economical for studying transition-metal complexes.

Experimental Section

The experiments for 120, 150, 223, and 293 K were carried out on a Siemens axs SMART CCD system with monocromated Mo Kα ($\lambda = 0.710\ 73$ Å) radiation. The data were collected over a hemisphere of reciprocal space, by a combination of sets. Each set had a different ϕ angle for the crystal, and each exposure of 64 s covered 0.25° in ω. The crystal to detector distance was 2.9 cm, coverage 99.7% of the unique set up to 56° in 2θ.

The collected frames were integrated using the preliminary cell-orientation matrix. The software SMART[25] was used for collecting the frame of data, indexing reflections, and determination of lattice parameters, SAINT[25] for integration of the intensity of reflection and scaling, and SADABS[26] for absorption correction. The program package used to solve and refine the structure, create the molecular graphics, and prepare the material for publication was SHELXTL-PC.[27] Final R (%) values are listed in Table 9.

(25) Siemens SMART and SAINT Area detector control and Integration software, Siemens Analytical X-ray Instrument Inc., Madison, WI, 1996.
(26) Sheldric, G. M. SADABS. Empirical Absorption Correction Program, University of Gottingen, Germany, 1996.
(27) Siemens SHELXTL Reference Manual, Analytical X-ray Instrument Inc., Madison, WI, 1994.

The structure was solved by direct methods. All non-hydrogen atoms were refined by full-matrix least-squares with an anisotropic temperature factor. The hydrogen atoms were included at idealized positions. The experiments were carried out two times, and the present work does not show the short bond distance for carbon atoms in one pyridine ring presented by Moreno-Esparza et al.[16] at low temperatures. The related parameters for the crystal at different temperatures are summarized in Table 10, and the molecular structure is illustrated in Figure 6.

Acknowledgment. We thank Dr. R. Cetina and Dr. Zongchao Jia for their critical readings of the manuscript. We are grateful to Dr. Rafael Moreno-Esparza of the Facultad de Quimica, UNAM, Mexico, for kindly supplying a sample of [Fe(tpen)]-$(ClO_4)_2 \cdot {}^2/_3H_2O$. The diffraction data have been collected on a Siemens-Bruker axs GmbH, Karlsruhe, FRG, by Dr. Eric Hovestreydt, who we thank for his generous support. This work was financially supported by the Universidad Nacional Autonoma de Mexico, NSFC (Grant 29992590-1) and the Ministry of Education in China.

IC990676Z